applied sciences

MDPI

Article

An Experimental Validated Control Strategy of Maglev Vehicle-Bridge Self-Excited Vibration

Lianchun Wang [1], Jinhui Li [1,2], Danfeng Zhou [1] and Jie Li [1,*]

1 College of Mechatronics Engineering and Automation, National University of Defense Technology, Changsha 410073, China; spring_512@163.com (L.W.); li_jinhui@126.com (J.L.); zdfnudt@163.com (D.Z.)
2 Scinence and Technology on Near-Surface Detection Laboratory, Wuxi 214035, China
* Correspondence: jieli@nudt.edu.cn; Tel.: +86-731-845-73388 (ext. 8103)

Academic Editors: Gangbing Song, Steve C.S. Cai and Hong-Nan Li
Received: 12 October 2016; Accepted: 23 December 2016; Published: 4 January 2017

Abstract: This study discusses an experimentally validated control strategy of maglev vehicle-bridge vibration, which degrades the stability of the suspension control, deteriorates the ride comfort, and limits the cost of the magnetic levitation system. First, a comparison between the current-loop and magnetic flux feedback is carried out and a minimum model including flexible bridge and electromagnetic levitation system is proposed. Then, advantages and disadvantages of the traditional feedback architecture with the displacement feedback of electromagnet y_{E} and bridge y_{B} in pairs are explored. The results indicate that removing the feedback of the bridge's displacement y_{B} from the pairs ($y_{\mathrm{E}} - y_{\mathrm{B}}$) measured by the eddy-current sensor is beneficial for the passivity of the levitation system and the control of the self-excited vibration. In this situation, the signal acquisition of the electromagnet's displacement y_{E} is discussed for the engineering application. Finally, to validate the effectiveness of the aforementioned control strategy, numerical validations are carried out and the experimental data are provided and analyzed.

Keywords: maglev; levitation system; bridge; self-excited vibration; energy

1. Introduction

Compared with the traditional railway train system, the electromagnetic maglev system has advantages of less exhaust fumes emission, lower noise and the ability to climb steeper slopes, which has attracted wide attention in recent years [1–3].

Maglev's rapid development and its potential commercial applications depict a bright future. However, there are still some issues to be solved urgently, such as the vehicle-bridge stationary self-excited vibration [4,5]. When the maglev train is suspended on some special bridges with minor weight per meter, the maglev train and bridges may vibrate vertically and continuously, which degrade the stability of the levitation control and the ride comfort.

In magnetic engineering, due to its clear physical meaning and excellent performance, the cascaded-loop control architecture with displacement-loop and current-loop to control the electromagnetic force is widely adopted [6,7]. According to the formulation of the electromagnetic force, the electromagnetic force is related to the levitation gap and current. To some extent, the electromagnetic force, the levitation gap and the current are interactive and complex. As we all know, from the perspective of the magnetic flux, the electromagnetic force is solely determined by the magnetic flux [8]. The relationship between the electromagnetic force and magnetic flux is simple and clear, if the magnetic flux-loop instead of the traditional current-loop is adopted to control the electromagnetic force, it may be favorable for the stabilization of interaction system. Hence, the magnetic flux will be discussed and adopted in this paper.

To master the underlying principles of the self-excited vibration, plenty of studies have been carried out from different perspectives. Albert et al. [9,10] pointed out that the American magnetic levitation system was successfully suspended in Florida, but it was incapable of achieving stable suspension when the vehicle was moved to the old Dominican university campus. They believed that the over-flexibility of the latter bridge was the main reason for the difficulties of stable suspension.

Wang et al. believed that the self-excited vibration is caused by the inappropriate frequency relationship between the various components of the Maglev vehicle-bridge interaction system [11]. Therefore, the proper frequency distribution is an effective strategy to avoid the resonance. The center manifold method was carried out to discuss the underlying principles of the self-excited vibration in the literature [12,13]. It is believed that the self-excited vibration results from the bifurcations and chaos.

The aforementioned studies about the roots of the self-excited vibration provide us inspiration to avoid the vibration. In this paper, based on the proposed minimum model, the underlying principles of the self-excited vibration will be explored from the real parts of its characteristic roots.

To eliminate the self-excited vibration, the methods, including optimization of the parameters and minimization of the time-delay of feedback channels [14], virtual tuned mass damper algorithm [15] and the virtual energy harvester algorithm [16] are explored by different scholars. They believed that these control strategies can avoid the self-excited vibration for the given bridge. Yau intends to develop a neuro-PI (proportional-integral) controller to control the dynamic response of the maglev vehicles around an allowable prescribed acceleration, numerical simulations demonstrate that a trained neuro-PI controller has the ability to control the acceleration amplitude for running maglev vehicles [17]. However, due to the complexity, the robustness to bridges with different modal frequencies awaits further research.

In this paper, by the analysis of the block diagrams in depth, we find that removing the displacement feedback of bridge instead of the feedback in pairs is an effective technique to enable levitation subsystem passivity and to solve the problem of self-excited vibration theoretically. Furthermore, several implementation issues, including the estimation of bridge's displacement are addressed.

The purpose of the research reported here is to develop a vibration control method that can eliminate the self-excited vibration, and is suitable for the magnetic levitation system.

2. Modeling of Vehicle-Bridge Interaction

Generally, the choice of model's complexity of the maglev vehicle-bridge system depends on its usage. For the validation by the numerical simulation, the model should be precise enough to improve the creditability and precision. For the exploration of the principle and the design of control strategy, the minimum interaction model containing the quintessential parts, a flexible bridge and a levitation unit, may be more practical and effective.

In this section, the nonlinear part of the bridge is ignored because the magnitude of the self-vibration is small enough when compared to the span of the bridge. Furthermore, the bridge is simplified as a Bernoulli–Euler beam because the other dimensions of bridges are much smaller than its length. In addition, the electromagnetic force acting on the bridge and electromagnet is regarded as an equivalent concentrated force. Furthermore, the kinetics coupling between adjacent levitation units and the influence of air springs are neglected [16].

2.1. Modeling of Bridge

Based on the above assumptions, the minimum interaction model is shown in Figure 1. The variables y_{B} and y_{E} are the vertical displacements of bridge and electromagnet, respectively. The variable δ is the levitation gap measured by the gap sensor, and m_{E} is the equivalent mass of electromagnet.

The motion of bridge is described by the following differential equation [4]:

$$EI_{\mathrm{B}}\frac{\partial^4 y_{\mathrm{B}}(x,t)}{\partial x^4}+\rho_{\mathrm{B}}\frac{\partial^2 y_{\mathrm{B}}(x,t)}{\partial t^2}=f(x,t) \tag{1}$$

where the variable x is the axial coordinate of the bridge, t is the time, EI_B is the bending rigidity, ρ_B is the mass per unit length, and $f(x,t)$ is the electromagnetic force acting on the bridge.

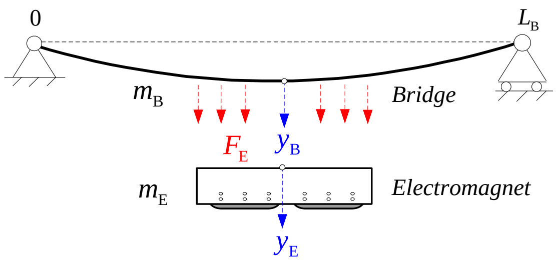

Figure 1. The minimum model of Maglev vehicle-bridge system. Red arrows: F_E is electromagnetic force; blue arrows: y_B and y_E are the vertical displacements of bridge and electromagnet.

For a simply supported bridge, the first modal frequency ω_B and modal shape functions $\phi_B(x)$ are

$$\omega_B = \lambda_B^2 \sqrt{EI_B/\rho_B} \tag{2}$$

$$\phi_B(x) = \sin(\lambda_B x) \tag{3}$$

where λ_B is the space wavelength of the bridge's first modal, and $\lambda_B = \pi/L_B$. The fact observed from the maglev base of china shows that the self-excited vibration is mainly aroused by the first modal of bridges. Hence, in this section, the first modal of bridge is considered solely. Thus, the solutions of Equation (1) may be expressed as

$$y_B(x,t) = \phi_B(x) q_B(t) \tag{4}$$

where $q_B(t)$ is the time-varying amplitude of the modal displacement. Substituting the Equation (4) into Equation (1), multiplying both sides of the aforementioned resultant equation by $\phi_k(x)$, then integrating both sides from 0 to L_B gives

$$\ddot{q}_B(t) + 2\xi_B\omega_B\dot{q}_B(t) + \omega_B^2 q_B(t) = 2\rho_B^{-1}L_B^{-1}\sum_{i=1:n}\phi_B(x_i)F_{Ei}(t) \tag{5}$$

where n is the number of levitation units suspended on a single bridge. Multiplying both sides of the resultant equation by $\phi_B(x)$ gives

$$\ddot{y}_B(x,t) + 2\xi_B\omega_B\dot{y}_B(x,t) + \omega_B^2 y_B(x,t) = 2m_B^{-1}\phi_B(x)\cdot\sum_{i=1:n}\phi_B(x_i)F_{Ei}(t) \tag{6}$$

where $m_B = \rho_B L_B$ is the total mass of bridge. The phases of electromagnetic forces $F_{Ei}(t)(i = 1:n)$ are exactly in concert and the amplitude of $F_{Ei}(t)$ is proportional to the value of $\phi_B(x_i)$ when the self-excited vibration occurs with the first-order modal frequency [18]. As for Equation (6), with regard to the special case $x = 0.5L_B$, it gives that

$$\ddot{y}_B(t) + 2\xi_B\omega_B\dot{y}_B(t) + \omega_B^2 y_B(t) = \sigma m_B^{-1} F_E(t) \tag{7}$$

where $\sigma = 2\sum_{i=1:n}\phi_B^2(x_i)$, the variable $y_B(t)$ is the modal displacement and the variable $F_E(t)$ is the electromagnetic force of the levitation unit at the location of $x = 0.5L_B$. Equation (7) may be considered as the response of bridge roused by the electromagnetic force $F_E(t)$.

2.2. Modeling of Levitation System

Suppose the turns of a single electromagnet is N, the pole area is A, and the magnetic permeability of vacuum is μ_0. Then, for a single electromagnet [3], the balance equations of electromagnetic force $F_E(t)$ and voltage $u(t)$ are

$$\begin{cases} F_E(t) = \frac{\mu_0 A N^2}{2}\left(\frac{i(t)}{\delta(t)}\right)^2 \\ 2Ri(t) + \frac{\mu_0 A N^2}{\delta(t)}\dot{i}(t) - \frac{\mu_0 A N^2 i(t)}{\delta^2(t)}\dot{\delta}(t) = u(t) \end{cases} \tag{8}$$

where R is the resistance, $i(t)$ is the current of electromagnet. In light of Equation (8), the balance equation of voltage is related with the four variables, control voltage $u(t)$, current $i(t)$, levitation gap $\delta(t)$ and its derivative $\dot{\delta}(t)$. Besides, the value of $F_E(t)$ refers to the two variables, current $i(t)$ and levitation gap $\delta(t)$.

To simplify the above relationship, the magnetic flux $B(t)$ instead of the current $i(t)$ may be adopted when developing the dynamic equations. In this way, Equation (8) is updated as

$$\begin{cases} F_E(t) = \frac{2A}{\mu_0}B^2(t) \\ 2NA\dot{B}(t) + \frac{4R}{\mu_0 N}\delta(t)B(t) = u(t) \end{cases} \tag{9}$$

In light of Equation (9), it can be seen that the balance equation of voltage is related with three variables and the electromagnetic force is solely determined by the magnetic flux. Compared with Equation (8), the dynamic equation is much simpler and clearer, which may be favorable adopted for the synthesis of the vehicle-bridge interaction system.

Generally, the natural frequency of air springs is far less than the bandwidth of the levitation control system and the modal frequencies of bridges, so the dynamics of sprung mass is neglected. Combining Equation (7), the movement of electromagnet is

$$m_E\ddot{y}_E(t) = -F_E(t) + (m_C + m_E)g \tag{10}$$

where the variable $y_E(t)$ is the vertical displacement of electromagnet, g is the acceleration of gravity, m_C is the sprung mass, and m_E is the mass of electromagnet. According to Equations (9) and (10), it can be seen that the steady voltage of electromagnet is

$$u_0 = 2R\delta_0\sqrt{2(m_C + m_E)g/(\mu_0 N^2 A)} \tag{11}$$

where the variable δ_0 is the desired clearance between the upper surface of the electromagnet and the lower surface of the guideway.

Traditionally, the cascade control, the inner-loop with current feedback, the outer-loop with states feedback (proportion, damping and acceleration feedback) is widely adopted in maglev engineering. It gives that

$$u(t) = k_c\left[i_{\exp}(t) - i(t)\right] + u_0 \tag{12}$$

$$i_{\exp}(t) = k_p e(t) + k_d\dot{y}_E(t) + k_a\ddot{y}_E(t) \tag{13}$$

where the variable $i_{\exp}(t)$ is the desired current of electromagnet and the error $e(t)$ of levitation gap is set as

$$e(t) = y_E(t) - y_B(t) - \delta_{set} \tag{14}$$

where δ_{set} is the expected levitation gap. To stabilize the maglev vehicle-bridge interaction system with magnetic flux feedback, a similar cascade control scheme, the inner-loop with magnetic flux feedback, the outer-loop with states feedback, is adapted, which gives

$$u(t) = k_B\left[B_{\exp}(t) - B(t)\right] + u_0 \tag{15}$$

$$B_{\exp}(t) = k_p e(t) + k_d\dot{y}_E(t) + k_a\ddot{y}_E(t) \tag{16}$$

where $B_{\exp}(t)$ is the desired magnetic flux of levitation gap. To draw the main innovation of this work, combining with Equation (14), Equations (13) and (16) may be rewritten as Equation (17) when the parameter $\overline{k}_p$ is equal to parameter k_p.

$$\begin{cases} i_{\text{exp}}(t) = k_{\text{p}} y_{\text{E}}(t) + k_{\text{d}} \dot{y}_{\text{E}}(t) + k_{\text{a}} \ddot{y}_{\text{E}}(t) - \bar{k}_{\text{p}} y_{\text{B}}(t) - k_{\text{p}} \delta_{\text{set}} \\ B_{\text{exp}}(t) = k_{\text{p}} y_{\text{E}}(t) + k_{\text{d}} \dot{y}_{\text{E}}(t) + k_{\text{a}} \ddot{y}_{\text{E}}(t) - \bar{k}_{\text{p}} y_{\text{B}}(t) - k_{\text{p}} \delta_{\text{set}} \end{cases} \tag{17}$$

Thus, the minimum vehicle-bridge interaction model with active control is developed.

3. Principle of Self-Excited Vibration

It has been observed that when the maglev vehicle is suspended on the bridge staying still or moving slowly, the self-excited vibration occurs. When the vibration amplitude of bridge is sufficiently small, the interaction system is quasi-static. Hence, the linearized model is practical to simplify the analysis process without introducing noticeable errors.

Combining Equations (7) and (10) in time domains [18], the vertical dynamics of electromagnet and bridge in frequency domains can be converted to

$$\begin{cases} -m_{\text{E}} s^2 y_{\text{E}}(s) = F_{\text{E}}(s) \\ \sigma^{-1} m_{\text{B}} (s^2 + 2\xi_{\text{B}} \omega_{\text{B}} + \omega_{\text{B}}^2) y_{\text{B}}(s) = F_{\text{E}}(s) \end{cases} \tag{18}$$

Similarly, when the magnetic flux inner-loop is adopted, Combining Equations (9), (15) and (16) in time domains, the electromagnetic force and balance equation of voltage in frequency domains can be converted to

$$\begin{cases} F_{\text{E}}(s) = k_{\text{F}} B(s) \\ B(s) = \left((k_{\text{p}} k_{\text{B}} + k_{\text{d}} k_{\text{B}} s + k_{\text{a}} k_{\text{B}} s^2) y_{\text{E}}(s) - \bar{k}_{\text{p}} k_{\text{B}} y_{\text{B}}(s) \right) / (2NAs + k_{\text{B}}) \end{cases} \tag{19}$$

Combining Equations (18) and (19), the maglev vehicle-bridge interaction system may be represented by the following block diagram in Figure 2, where the electromagnetic module (*EM)* block is the voltage equation shown by Equation (9).

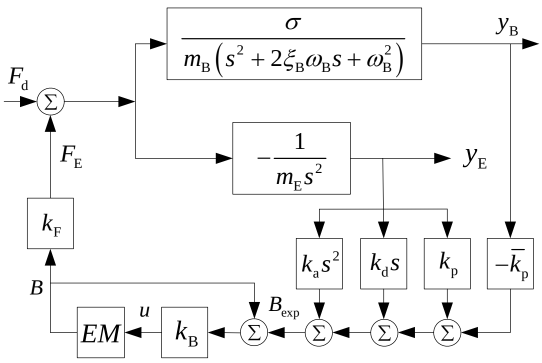

Figure 2. The equivalent block diagram of maglev vehicle-bridge system.

3.1. Stability of Levitation System

The stability of the levitation subsystem itself is a precondition for the avoidance of the maglev vehicle-bridge self-excited vibration. When studying the stability of the levitation system itself, the vertical displacement of bridge y_{B} is set as zero. In this case, the transfer function from the disturbance F_{d} to the displacement y_{E} of electromagnet is

$$T_1(s) = \frac{y_{\text{E}}(s)}{F_{\text{d}}(s)} = \frac{G_{\text{E}}(s)}{1 - G_{\text{E}}(s) H_{\text{E}}(s)} \tag{20}$$

where

$$\begin{cases} G_{\text{E}}(s) = -\frac{1}{m_{\text{E}} s^2} \\ H_{\text{E}}(s) = \frac{k_{\text{B}} k_{\text{F}}}{2NAs + k_{\text{B}}} (k_{\text{a}} s^2 + k_{\text{d}} s + k_{\text{p}}) \end{cases} \tag{21}$$

The characteristic equation of the transfer function $T_1(s)$ is

$$\Delta_1 = 2NAm_E s^3 + (m_E k_B + k_B k_F k_a)s^2 + k_B k_F k_d s + k_B k_F k_p \tag{22}$$

For the levitation subsystem, the parameters k_p, k_d, k_a, k_B are positive and adjustable, and $k_F = 4AB_0/\mu_0$. According to the Routh–Hurwitz stability criterion, the levitation subsystem is stable when Equation (23) is satisfied.

$$(m_E k_B + k_B k_F k_a)k_d > 2NAm_E k_p \tag{23}$$

3.2. Stability of Vehicle-Bridge Interaction System

To study the stability of the maglev vehicle-bridge interaction system, the transfer function from disturbance F_d to the displacement y_B of bridge should be calculated again when the displacement of bridge y_B is considered. In light of Figure 2, it gives that

$$T_2(s) = \frac{G_B(s)}{1 - G_E(s)H_E(s) - G_B(s)H_B(s)} \tag{24}$$

where

$$\begin{cases} G_B(s) = \frac{\sigma}{m_B\left(s^2+2\xi_B\omega_B s+\omega_B^2\right)} \\ H_B(s) = -\frac{k_B k_F}{2NAs+k_B}\cdot \bar{k}_p \end{cases} \tag{25}$$

Combining Equations (21), (24) and (25), the characteristic equation of the interaction system is

$$a_5 s^5 + a_4 s^4 + a_3 s^3 + a_2 s^2 + a_1 s + a_0 = 0 \tag{26}$$

where $a_5 = 2NAm_B m_E$, $a_4 = m_B m_E(k_B + 4NA\xi_B\omega_B) + k_B k_F m_B k_a$, $a_3 = m_B m_E\left(2k_B\xi_B\omega_B + 2NA\omega_B^2\right) + k_B k_F m_B(2k_a\xi_B\omega_B + k_d)$, $a_2 = k_B\omega_B^2 m_B m_E + \sigma m_E k_B k_F \bar{k}_p + k_B k_F m_B\left(k_p + 2k_d\xi_B\omega_B + k_a\omega_B^2\right)$, $a_1 = k_B k_F m_B\left(k_d\omega_B^2 + 2k_p\xi_B\omega_B\right)$, and $a_0 = k_B k_F m_B k_p\omega_B^2$. Generally, the roots of Equation (26) are calculable provided that the parameters are definite, which are denoted as $x_{1,2} = R_1 \pm jI_1$, $x_{3,4} = R_2 \pm jI_2$ and $x_5 = R_3$. If the three real parts R_1, R_2 and R_3 all are negative, the interaction system is stable and the self-excited vibration is avoided.

However, the stability of the interaction system is closely related with the bridge's modal frequency ω_B. To illustrate this, the parameters of interaction system are set as $k_p = 1000$, $k_d = 30$, $k_a = 0.4$, $k_B = 30$, $N = 360$, $A = 0.01848$, $\xi_B = 0.005$, and $B_0 = 0.6193$.

According to Equations (15) and (17), the traditional cascade control is adopted when the parameters $\bar{k}_p$ is set as the same with k_p. This is to say, $\bar{k}_p = 1000$. In this case, the real parts R_1, R_2 and R_3 associated with the modal frequency ω_B are shown in Figure 3.

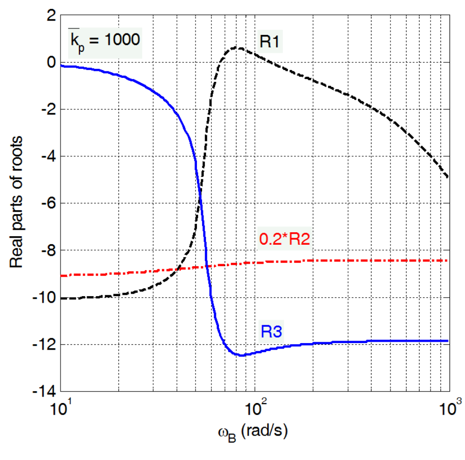

Figure 3. The real parts of characteristic roots for the standard cascade control.

According to Figure 3, it can be seen that the real parts of R_2 and R_3 are negative from 0 to 1000 rad/s. However, the value of R_1 is positive when the modal frequency ω_B belongs to the interval 67.3–118.7 rad/s. This is to say, the interaction system is unstable when the modal frequency ω_B belongs to the interval 67.3–118.7 rad/s. The self-excited vibration will appear.

To avoid the self-excited vibration, tuning the control parameters k_p, k_d, k_a and k_B is an effective technique. However, the ranges of parameters are limited by the performance specification of the levitation subsystem and the noise level of corresponding signals. Hence, a more feasible and robust method should be developed.

3.3. Principle of Self-Excited Vibration from the Perspective of Energy Interchange

From the quiescent state to the vibration state, the bridge needs to absorb energy. However, the interaction system only consists of the electromagnetic levitation system and bridge, so the absorbed energy by bridge is from the exportation of levitation system. Therefore, the characteristic of the energy exportation of the levitation system may be decisive for the occurrence of the self-excited vibration. In this section, we try to discuss the principle of self-excited vibration from the perspective of energy interchange between the bridge subsystem and levitation subsystem.

It has been found that when the vehicle is suspended on some special bridges, standing still or moving under 10 km/h, the self-excited vibration may appear and grow up continuously. Even so, at the beginning of the self-excited vibration, the amplitude of the vibration is tiny enough. In this case, the interaction system may be seen as quasi-static.

When studying the stability of the interaction system around the equilibrium point at the quasi-static states, the analysis process can be simplified by a linearization model without introducing significant errors. Linearizing Equations (8), (10) (13) and (14), the linearized system of frequency domain is given by

$$\begin{cases} u(s) = 2L_0 s i(s) + 2Ri(s) - 2F_i s y_E(s) + 2F_i s y_B(s) \\ F_E(s) = 2F_i i(s) - 2F_z y_E(s) + 2F_z y_B(s) \\ F_E(s) = -m_E s^2 y_E(s) \\ u(s) = k_c(k_p + k_d s + k_a s^2) y_E(s) - k_p k_c y_B(s) - (k_c - 2R) i(s) \end{cases} \tag{27}$$

where $L_0 = 0.5\mu_0 A N^2 z_0^{-1}$, $F_i = 0.5\mu_0 A N^2 i_0 z_0^{-2}$, $F_z = 0.5\mu_0 A N^2 i_0^2 z_0^{-3}$. Eliminating the variables $u(s)$, $i(s)$ and $y_E(s)$, the transfer function between $F_E(s)$ and $\dot{y}_B(s)$ is

$$H(s) = \frac{F_E(s)}{\dot{y}_B(s)} = -\frac{\eta_0 m_E s}{\eta_3 s^3 + \eta_2 s^2 + \eta_1 s + \eta_0} \tag{28}$$

where $\eta_0 = F_i k_c \left(k_p - i_0 z_0^{-1}\right)$, $\eta_1 = F_i k_c k_d$, $\eta_2 = 0.5 m_E k_c + F_i k_c k_a$, and $\eta_3 = m_E L_0$. The vibration frequency is assumed as ω_{Vib} and the velocity of the bridge is defined as $\dot{y}_B(t) = 0.1\cos(\omega_{Vib} t + \phi)$. According to Equation (28), the electromagnetic force working on the bridge is

$$F_E(t) = 0.1|H(j\omega_{Vib})|\cos(\omega_{Vib} t + \angle H(j\omega_{Vib})) \tag{29}$$

Furthermore, the averaged power of the electromagnetic force acting on the bridge is

$$P_E(\omega_{Vib}) = \frac{1}{T}\int_0^T F_E(\tau)\dot{y}_B(\tau)\mathrm{d}\tau = \frac{1}{200}\mathrm{Re}[H(j\omega_{Vib})] \tag{30}$$

Supposing the damping of bridge is viscous and linear, the damping force is

$$F_D(\omega_{Vib}, t) = 2\xi_k \omega_{Vib} m_B \dot{y}_B(\tau) \tag{31}$$

Herein the averaged power consumed by the damping is

$$P_{\mathrm{D}}(\omega_{\mathrm{Vib}}) = \frac{1}{T}\int_0^T F_{\mathrm{D}}(\omega_{\mathrm{Vib}}, \tau)\dot{y}_{\mathrm{B}}(\tau)\mathrm{d}\tau = 0.01\xi_k\omega_{\mathrm{Vib}}m_{\mathrm{B}} \tag{32}$$

The average power accumulated is

$$P_{\mathrm{B}}(\omega_{\mathrm{Vib}}) = P_{\mathrm{E}}(\omega_{\mathrm{Vib}}) - P_{\mathrm{D}}(\omega_{\mathrm{Vib}}) \tag{33}$$

In the normal case of equivalent parameters, the relationships between the vibration frequency and averaged powers are shown in Figure 4.

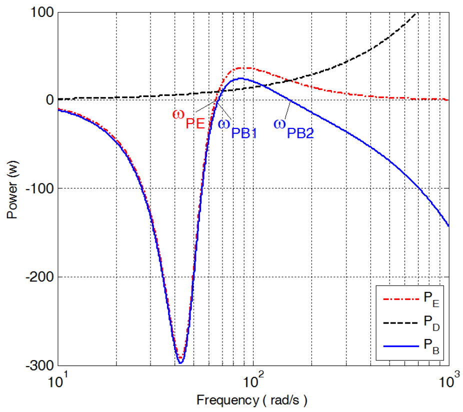

Figure 4. The averaged powers.

According Figure 4, for the crossover frequency $\omega_{\mathrm{P_E}}$, $P_{\mathrm{E}}(\omega_{\mathrm{P_E}}) = 0$. For any $\omega_{\mathrm{Vib}} < \omega_{\mathrm{P_E}}$, the averaged power $P_{\mathrm{E}}(\omega_{\mathrm{Vib}})$ working on the bridge is negative. This means that the levitation subsystem will absorb the vibration energy of the bridge subsystem when self-excited vibration occurs. On the contrary, for any $\omega_{\mathrm{Vib}} > \omega_{\mathrm{P_E}}$, the averaged power $P_{\mathrm{E}}(\omega_{\mathrm{Vib}})$ working on the bridge is positive. This means that when the self-excited vibration occurs, the levitation subsystem will export energy to the bridge subsystem.

For the bridge subsystem, the energy consumed by its modal damping should be considered. The modal damping attenuates the energy accumulation of the bridge subsystem. This is to say, the larger the modal damping ratio of bridge is, the more energy of bridge will be consumed, and the better the stability of the interaction system will be. However, the modal damping ratio of bridge is determined by its material, and the range is limited.

For any $\omega_{\mathrm{Vib}} \in \left(\omega_{\mathrm{PB1}} \quad \omega_{\mathrm{PB2}} \right)$, the bridge accumulates the averaged power $P_{\mathrm{B}}(\omega_{\mathrm{Vib}})$ that is positive. That is, the power consumed by the damping of the bridge is less than the power provided by the levitation subsystem. In this situation, the vibration energy of bridge accumulates and the amplitude of vibration increase continuously until the failure of suspension control.

For any $\omega_{\mathrm{Vib}} \notin \left(\omega_{\mathrm{PB1}} \quad \omega_{\mathrm{PB2}} \right)$, the averaged power $P_{\mathrm{B}}(\omega_{\mathrm{Vib}})$ is negative, which indicates that the vibration energy of bridge will decay to zero with the passage of time, and the self-excited vibration is avoided.

4. Suppression Strategy of Self-Excited Vibration

4.1. Influence on Stability with Regard to $\overline{k}_p$

According to Equation (17), the expected magnetic flux B_{exp} consists of the states (displacement y_{E}, velocity $\dot{y}_{\mathrm{E}}$ and acceleration $\ddot{y}_{\mathrm{E}}$) of levitation subsystem and the state (displacement y_{B}) of bridge subsystem.

In maglev engineering, the levitation eddy-current sensor can detect the relative displacement $(y_{\mathrm{E}} - y_{\mathrm{B}})$ between the upper surface of the electromagnet and the lower surface of the guideway.

However, the electromagnet's displacement y_E and bridge's displacement y_B can be measured independently. Traditionally, there is no choice but to feed back the displacement of electromagnet and bridge is in pairs $(y_E - y_B)$.

Up to now, no literature indicates that the displacement feedback in pairs is optimal for the levitation stability and the suppression of the self-excited vibration. Taking the stability condition of the levitation subsystem for example, according to the Equation (21), the stability of the levitation subsystem is uncorrelated with the feedback gain of the bridge's displacement $\bar{k}_p$.

Similarly, according to Figure 2, to some extent, the feedback of the bridge's displacement increases the complexity of the block diagram. Furthermore, its influence on the occurrence of the self-excited vibration is unclear and should be explored.

To study the influence on the stability of the interaction system with the feedback of the bridge's displacement $\bar{k}_p$, for an extreme case, we suppose that $\bar{k}_p = 0$. This is to say, the feedback path of the bridge's displacement is removed from traditional control framework. In this case, the block diagram of maglev vehicle-bridge system is updated as Figure 5.

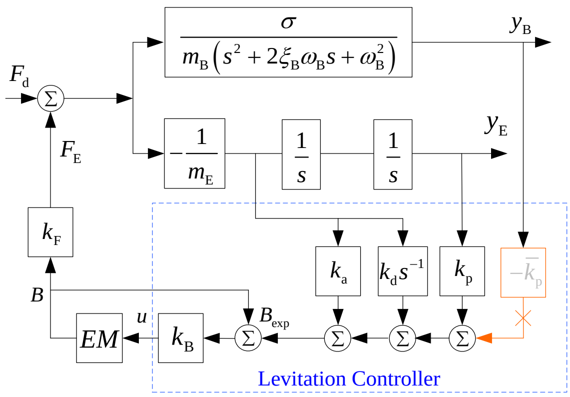

Figure 5. The block diagram of maglev vehicle-bridge system.

In light of Figure 5, the transfer function from disturbance F_d to the displacement y_B of bridge is degraded to

$$T_3(s) = \frac{G_B(s)}{1 - G_E(s)H_E(s)} \tag{34}$$

In this case, the characteristic equation of the transfer function $T_3(s)$ is

$$\Delta_3 = \Delta_1 \cdot \left(s^2 + 2\xi_B \omega_B s + \omega_B^2\right) \tag{35}$$

In light of Equation (35), the characteristic equation of the interaction system is the product of the characteristic polynomial of levitation system itself Δ_1 and $s^2 + 2\xi_B \omega_B s + \omega_B^2$.

Obviously, the characteristic polynomial $s^2 + 2\xi_B \omega_B s + \omega_B^2$ is stable. Hence, we can conclude that the interaction system is stable provided that the levitation subsystem is stable. This is to say, the stability of the interaction system is degenerated into the stability of the levitation subsystem. In this case, the self-excited vibration will be avoided if Equation (23) is satisfied.

To illustrate the conclusion quantitatively, the gain $\bar{k}_p$ is set as zero, and the other parameters are kept the same as the above section. The real parts of characteristic roots of the maglev vehicle-bridge interaction system are shown in Figure 6 when the modal frequency ω_B is varying.

In light of Figure 6, it can be seen that the real parts R_1, R_2 and R_3 are all negative when $\bar{k}_p = 0$. Hence, from the perspective of the characteristic roots, removing the bridge's displacement feedback is beneficial for the stability of the interaction system.

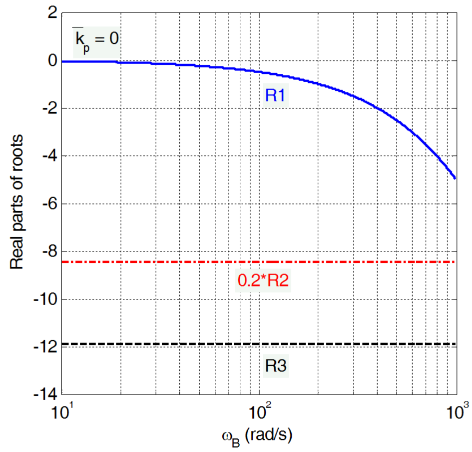

Figure 6. The real parts of characteristic roots when $\bar{k}_\mathrm{p} = 0$.

4.2. Energy Variation with Regard to $\bar{k}_p$

In this section, we try to illustrate the validity of the control strategy from the perspective of the energy variation. When the feedback gain of the bridge's displacement $\bar{k}_\mathrm{p}$ is set as zero, Equation (27) may be rewritten as

$$\begin{cases} u(s) = 2L_0 s i(s) + 2Ri(s) - 2F_\mathrm{i} s y_\mathrm{E}(s) \\ F_\mathrm{E}(s) = 2F_\mathrm{i} i(s) - 2F_\mathrm{z} y_\mathrm{E}(s) + 2F_\mathrm{z} y_\mathrm{B}(s) \\ F_\mathrm{E}(s) = -m_\mathrm{E} s^2 y_\mathrm{E}(s) \\ u(s) = k_\mathrm{c}(k_\mathrm{p} + k_\mathrm{d} s + k_\mathrm{a} s^2) y_\mathrm{E}(s) - (k_\mathrm{c} - 2R) i(s) \end{cases} \tag{36}$$

Based on Equation (36), the transfer function between $F_\mathrm{E}(s)$ and $\dot{y}_\mathrm{B}(s)$ is updated as

$$H(s) = \frac{F_\mathrm{E}(s)}{\dot{y}_\mathrm{B}(s)} = \frac{2F_\mathrm{z} m_\mathrm{E} s(2L_0 s + k_\mathrm{c})}{\eta_3 s^3 + \eta_2 s^2 + \eta_1 s + \eta_0} \tag{37}$$

where $\eta_0 = 2F_\mathrm{i} k_\mathrm{c} k_\mathrm{p} - 2F_\mathrm{z} k_\mathrm{c}$, $\eta_1 = 2F_\mathrm{i} k_\mathrm{c} k_\mathrm{d} - 4L_0 F_\mathrm{z} + 4F_\mathrm{i}^2$, $\eta_2 = m_\mathrm{E} k_\mathrm{c} + 2F_\mathrm{i} k_\mathrm{c} k_\mathrm{a}$, and $\eta_3 = 2m_\mathrm{E} L_0$. In the case of $\bar{k}_\mathrm{p} = 0$, the relationships between the vibration frequency and averaged powers are shown in Figure 7.

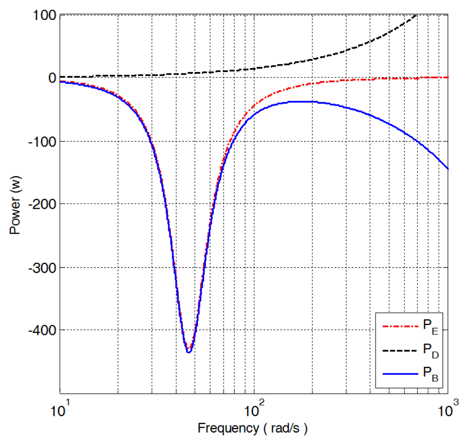

Figure 7. The averaged powers when $\bar{k}_\mathrm{p} = 0$.

According to Figure 7, it can be seen that the power P_E is negative over the full frequency range when the displacement feedback of bridge is removed. This is to say, the levitation subsystem is always passive if the feedback of the bridge's displacement y_B is removed. Furthermore, considering the passivity and the dissipation of bridge due to its modal damping, the vibration energy of bridge is delay to zero no matter how large the initial states are. In this case, the self-excited vibration is avoided.

4.3. The Estimation of Electromagnet's Displacement y_E

In an actual magnetic levitation system, there are two real-time signals available. The first signal is the levitation clearance $\delta(t) = y_E(t) - y_B(t)$, measured by the eddy-current sensor, and the other is the acceleration signal of the electromagnet $a_E(t) = \ddot{y}_E(t)$, detected by the accelerometer. Traditionally, the signal of levitation gap is adopted for the outer-loop of the levitation controller. Separately speaking, the feedback gain of the electromagnet's displacement y_E is k_p, and the feedback gain of the bridge's displacement are in pairs is $\bar{k}_p = -k_p$.

When the amplitude of the feedback gains of the electromagnet and bridge's displacement is different, i.e., $\bar{k}_p \neq -k_p$, we should measure the signal of electromagnet's displacement y_E and the bridge's displacement y_B separately. For a special case, $\bar{k}_p = 0$. We still should measure the signal of the electromagnet's displacement y_E.

Considering the signal of the electromagnet's displacement y_E is immeasurable directly, we should develop a method to estimate it. Theoretically, the displacement of electromagnet may be obtained by the double integration of acceleration of the electromagnet:

$$y_E(s) = \frac{1}{s^2} a_E(s) \tag{38}$$

However, in a real maglev system, measurements of acceleration $a_E(t)$ are polluted by its inexact direct bias and ultra low frequency disturbance, which will lead to integral saturation.

To prevent the integral saturation, the estimator $1/(s+\tau)^2$ is adopted to instead of the double-integrator $1/s^2$. This is to say, the estimated value $\hat{y}_E$ of the electromagnet's displacement is

$$\hat{y}_E(s) = \frac{1}{(s+\tau)^2} a_E(s) \tag{39}$$

where τ is the time constant of the estimator. The comparison between the double-integrator and the estimator is shown in Figure 8.

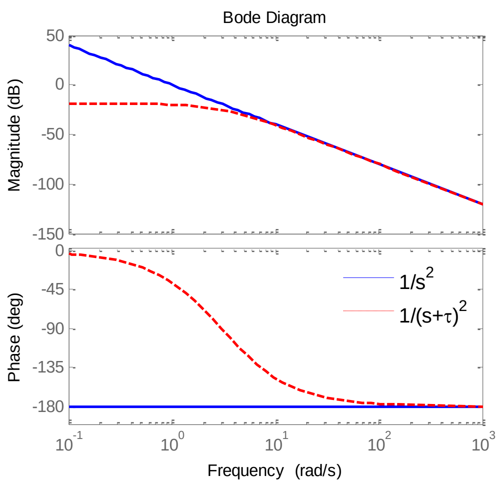

Figure 8. The comparison between the double-integrator and estimator.

Considering Figure 8, when the frequency is less than 10 rad/s, the amplitude of double-integrator is oversized, which may result in excessive transient response when the ultra-low frequency component of $a_E(t)$ is shifted. Hence, the double-integrator is unsuitable for the engineering application.

Luckily, compared with the double-integrator, the amplitude of the estimator is much smaller. Furthermore, when the frequency is larger than 10 rad/s, the amplitude and phase of estimator are highly consistent with the double-integrator, which provides enough phase advances over the upper frequency range. Therefore, compared with the double-integrator, the estimator is more suitable for the engineering applications. When the electromagnet's displacement y_{E} is replaced by the estimation one, the control Equation (17) is updated to Equation (40).

$$B_{\exp}(t) = k_{\mathrm{p}}\bar{y}_{\mathrm{E}}(t) + k_{\mathrm{d}}\dot{y}_{\mathrm{E}}(t) + k_{\mathrm{a}}\ddot{y}_{\mathrm{E}}(t) \tag{40}$$

However, the phase distortion of the estimator at the low frequency range, which may degrade the stability of the levitation system, should be considered. Generally, the larger the time constant τ is, the less the amplitude of the estimator will be at the ultra low frequency range, and the more seriously its phase distortion will be. Hence, the time constant τ should be selected comprehensively according to the amplitude elimination and phase distortion. When the estimator $1/(s+\tau)^2$ is adopted to replace the double-integrator $1/s^2$, the block diagram of maglev vehicle-bridge system is updated as Figure 9.

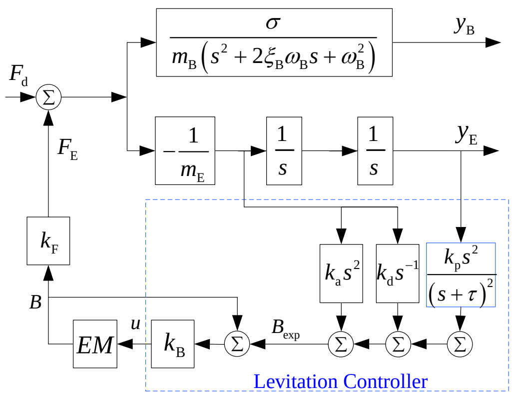

Figure 9. The block diagram of maglev vehicle-bridge system with estimator.

5. Numerical and Experimental Validation

Theoretically, the proposed control strategy can solve the problem of self-excited vibration effectively. Furthermore, it should be checked numerically and experimentally prior to applying to commercial service.

5.1. Numerical Validation

To obtain a reliable conclusion, the conditions of the magnetic levitation project should be simulated as precise as possible. In maglev engineering, the direct component of the acceleration signal is not absolute zero. Hence, its direct component is set as 0.2 m/s^2. The noise is set as 0.2% when compared to the maximum amplitude of the signal. Besides, the overall nonlinear dynamic model with details, which is shown in Figure 10, is adopted to carry out the numerical simulation. As for this model, ten modules (Due to the limit of Figure's size, only three modules is shown as follow.) are included and distributed along the length direction of the vehicle symmetrically. Each module consists of two levitation units.

During the process of simulation, the nonlinear character of the levitation system, the saturation of the control voltage of the electromagnets, the dynamic responses of air-springs, the real-time estimation of the signals of the electromagnet's displacement and the coupling between the adjacent levitation units are all considered.

In this subsection, the parameters of controller are set as $k_{\mathrm{p}} = 1000$, $k_{\mathrm{d}} = 30$, $k_{\mathrm{a}} = 0.4$, and $k_{\mathrm{B}} = 30$. The parameters of bridge are set as $\xi_{\mathrm{B}} = 0.005$, and $\omega_{\mathrm{B}} = 2\pi \times 13\mathrm{Hz} = 81.68$ rad/s.

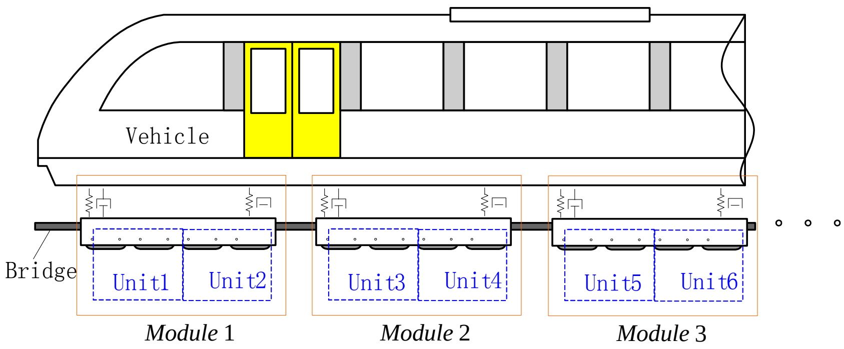

Figure 10. The overall nonlinear dynamic model with ten modules.

The modal frequency ω_B = 81.68 rad/s selected in this case belongs to the unstable interval 67.3–118.7 rad/s. As we expected, the self-excited vibration starts to grow up at t = 2 s. According to Figure 11b, it can be seen that the amplitude of the electromagnet's acceleration is up to 2 m/s^2, which indicates the electromagnet vibrates violently. The vibration of electromagnet will be transferred to the vehicle, which degrades its ride comfort. The fluctuation of electromagnet displacement is about 0.5 mm. The fluctuation impacts the durability and safety of the bridge.

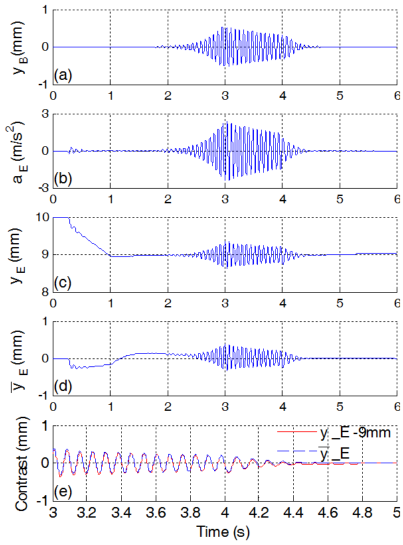

Figure 11. The numerical verification for vibration suppression method, which is activated at t = 4 s: (**a**) the displacement of bridge; (**b**) the displacement of electromagnet; (**c**) the estimated displacement of electromagnet, and (**d**) the contrast signals of the estimated and the real displacement of electromagnet.

According to Figure 11d, it can be seen that the estimated displacement of electromagnet is unfaithful when $t < 2$ s, which is due to the displacement estimator's transient response. In light of Figure 11e, when the transient response disappears, the estimated signal is converged to the real signal of electromagnet's displacement. To show its validity, the improved control scheme is activated at t = 4 s. It can be seen that the vibration amplitudes of all states rapidly decay to zero. When $t > 4.5$ s, the self-excited vibration disappears absolutely.

5.2. Experimental Validation

The experiments were carried out on the maintenance platform of the Tangshan maglev test line, as shown in Figure 12. The levitation control system (Beijing Enterprises Holdings Maglev Technology Development Co., Ltd, Beijing, China) consists of a Pulse Width Modulation(PWM) chopper, suspension modules and Power PC-based digital processor. The digital process is capable of performing the proposed vibration control algorithm.

Figure 12. Field experiments on a full-scale maglev train at Tangshan maglev engineering experiment base.

All experimental data were obtained from the monitoring terminal of the notebook computer and the Ethernet-based suspension monitoring network. The data sampling rate was 200 samples per second. The whole weight of the vehicle is 8 ton during experiment.

The full-scale maglev train consists of ten modules, ten air-springs and one cabin. The ten modules are distributed along the length direction of the vehicle symmetrically. For the bridge subsystem, the length of bridge is 18 m, and its mass per meter is about 2.4 ton. The field measurement indicates that its modal damping ratio is about 0.02. Considering the accuracy and reliability of the numerical model in Section 5.1 is close to the real maglev system, we expected the conclusion obtained by the numerical simulation to be validated by the field experiment.

Figure 13 shows the results of self-excited vibration when performing field tests on a maintenance platform. The self-excited vibration appeared when $t < 1$ s. It can be found that the signals of acceleration, levitation gap and current fluctuate violently. The electromagnet vibration degraded the stability of the suspension control and ride comfort of vehicle.

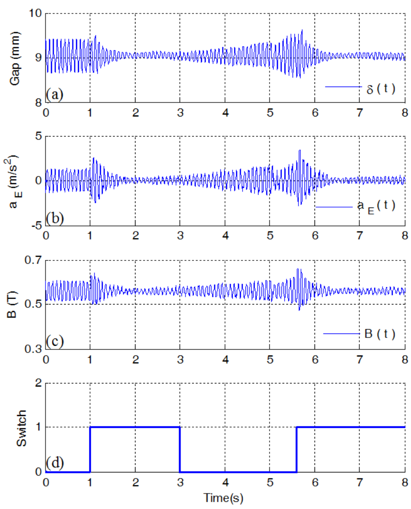

Figure 13. The experimental verification for vibration suppression method, which is activated during [1 3] and [5.5 8]: (**a**) the levitation gap; (**b**) the acceleration of electromagnet; (**c**) the magnetic flux; and (**d**) the switch signal.

At $t = 1$ s, the proposed control strategy was activated. After a short regulation, the signal's fluctuation of the levitation gap and the acceleration of electromagnet were attenuated greatly.

At t = 3 s, the control scheme was switched to the traditional cascaded-controller, the self-excited vibration aroused gradually. At t = 5.5 s, the control scheme was switched to proposed control strategy again, and the resonance disappear once more.

According to Figures 11 and 13, both the results of the numerical simulation and field experiment indicate that the proposed control scheme is capable of weakening the amplitude of the self-excited vibration to zero in two seconds.

At the same time, we also find that the experimental signals are much more irregular when compared with the signals obtained by the numerical simulation, which mainly results from the high-frequency noise from the eddy-current sensors and the inconsistent between the adjacent levitation units.

6. Conclusions

Firstly, the maglev vehicle-bridge interaction model, including a flexible bridge and several electromagnetic levitation units is proposed, and the comparison between the current-loop and magnetic flux feedback is carried out. The analysis indicated that the performance could be improved by substituting the current-loop with the magnetic flux-loop.

Secondly, the advantages and disadvantages of the traditional control architecture with the displacement feedback of electromagnet y_E and bridge y_B in pairs are explored. The results indicate that removing the feedback of the bridge's displacement y_B from the pairs $(y_E - y_B)$ measured by the eddy-current sensor is beneficial for the suppression of the self-excited vibration.

Thirdly, the signal acquisition of the electromagnet's displacement y_E is discussed for the engineering application. The analysis shows that the proposed estimation can avoid the problem of the integral saturation.

At last, the numerical research and the experimental validations on a full-scale maglev train at Tangshan maglev engineering experiment base have been carried out. The data indicated that the proposed control strategy is capable of eliminating the self-excited vibration.

Acknowledgments: This work was financially supported in part by the National Natural Science Foundation of China under Grant 112002230 and Grant 11302252. The authors would like to thank all reviewers for their valuable comments.

Author Contributions: Lianchun Wang and Jie Li proposed the new ideas and designed the experiments; Lianchun Wang performed the experiments; Lianchun Wang, Jinhui Li and Danfeng Zhou analyzed the data; and Lianchun Wang and Jinhui Li wrote the paper.

Conflicts of Interest: The authors declare no conflict of interest.

References

1. Zhou, H.B.; Duan, J.A. A novel levitation control strategy for a class of redundant actuation maglev system. *Control Eng. Pract.* **2011**, *19*, 1468–1478. [CrossRef]
2. Huang, C.M.; Yen, J.Y.; Chen, M.S. Adaptive nonlinear control of repulsive maglev suspension systems. *Control Eng. Pract.* **2000**, *8*, 1357–1367. [CrossRef]
3. Li, J.H.; Li, J. A practical robust nonlinear controller for maglev levitation system. *J. Cent. South Univ. Technol.* **2013**, *20*, 2991–3001. [CrossRef]
4. Li, J.H.; Li, J.; Zhou, D.F.; Yu, P.C. Self-excited vibration problems of maglev vehicle-bridge interaction system. *J. Cent. South Univ. Technol.* **2014**, *21*, 4184–4192. [CrossRef]
5. Zhou, D.F.; Li, J.; Hansen, C.H. Suppression of the stationary maglev vehicle-bridge coupled resonance using a tuned mass damper. *J. Vib. Control* **2013**, *19*, 191–203. [CrossRef]
6. Li, J.H.; Li, J.; Yu, P.C.; Wang, L.C. Adaptive backstepping control for levitation system with load uncertainties and external disturbances. *J. Cent. South Univ. Technol.* **2014**, *21*, 4478–4488. [CrossRef]
7. Glück, T.; Kemmetmüller, W.; Tump, C.; Kugi, A. A novel robust position estimator for self-sensing magnetic levitation systems based on least squares identification. *Control Eng. Pract.* **2011**, *19*, 146–157. [CrossRef]

8. Zhang, W.Q.; Li, J.; Zhang, K.; Cui, P. Stability and bifurcation in magnetic flux feedback maglev control system. *Math. Probl. Eng.* **2013**, *2013*, 537359. [CrossRef]
9. Alberts, T.E.; Hanasoge, A.; Oleszczuk, G. Stable levitation control of magnetically suspended vehicles with structural flexibility. In Proceedings of the 2008 American Control Conference, Seattle, WA, USA, 11–13 June 2008.
10. Alberts, T.E.; Oleszczuk, G. On the influence of structural flexibility on feedback control system stability for EMS Maglev vehicles. In Proceedings of the 19th International Conference on Magnetically Levitated Systems and Linear Drives, Dresden, Germany, 13–15 September 2006.
11. Wang, H.P.; Li, J. Vibration analysis of the maglev guideway with the moving load. *J. Sound Vib.* **2007**, *305*, 621–640. [CrossRef]
12. Zhang, Z.; Zhang, L. Hopf bifurcation of time-delayed feedback control for maglev system with flexible guideway. *Appl. Math. Comput.* **2013**, *219*, 6106–6112. [CrossRef]
13. Wang, H.P.; Li, J.; Zhang, K. Sup-resonant response of a non-autonomous maglev system with delayed acceleration feedback control. *IEEE Trans. Magn.* **2008**, *44*, 2338–2350. [CrossRef]
14. Zhou, D.F.; Hansen, C.H.; Li, J. Suppression of maglev vehicle-girder self-excited vibration using a virtual tuned mass damper. *J. Sound Vib.* **2011**, *330*, 883–901. [CrossRef]
15. Li, J.H.; Li, J.; Zhou, D.F.; Wang, L.C. The modeling and analysis for the self-excited vibration of the maglev vehicle-bridge interaction system. *Math. Probl. Eng.* **2015**, *2015*, 709583. [CrossRef]
16. Li, J.H.; Li, J.; Zhou, D.F.; Cui, P.; Wang, L.C.; Yu, P.C. The active control of maglev stationary self-excited vibration with a virtual energy harvester. *IEEE Trans. Ind. Electron.* **2015**, *62*, 2942–2951. [CrossRef]
17. Yau, J.D. Vibration control of maglev vehicles traveling over a flexible guideway. *J. Sound Vib.* **2009**, *321*, 184–200. [CrossRef]
18. Li, J.H.; Fang, D.; Zhang, D.; Cai, Y.; Ni, Q.; Li, J. A practical control strategy for the maglev self-excited resonance suppression. *Math. Probl. Eng.* **2016**, *2016*, 8071938. [CrossRef]